Reaction of Hydroxyl Radicals with Azacytosines: A Pulse Radiolysis and Theoretical Study

G. Pramod,[†] K. P. Prasanthkumar,[†] Hari Mohan,[‡] V. M. Manoj,[†] P. Manoj,[†] C. H. Suresh,*[,§] and C. T. Aravindakumar*[,†]

School of Chemical Sciences, Mahatma Gandhi University, Kottayam 686560, India, Radiation Chemistry and Chemical Dynamics Division, Bhabha Atomic Research Centre, Mumbai 400085, India, and Computational Modeling and Simulation Section, Regional Research Laboratory (CSIR), Trivandrum 695019, India

Received: June 24, 2006; In Final Form: August 6, 2006

Pulse radiolysis and density functional theory (DFT) calculations at B3LYP/6-31+G(d,p) level have been carried out to probe the reaction of the water-derived hydroxyl radicals (•OH) with 5-azacytosine (5Ac) and 5-azacytidine (5Acyd) at near neutral and basic pH. A low percentage of nitrogen-centered oxidizing radicals, and a high percentage of non-oxidizing carbon-centered radicals were identified based on the reaction of transient intermediates with 2,2′-azinobis(3-ethylbenzothiazoline-6-sulfonate), $ABTS^{2-}$. Theoretical calculations suggests that the N3 atom in 5Ac is the most reactive center as it is the main contributor of HOMO, whereas C5 atom is the prime donor for the HOMO of cytosine (Cyt) where the major addition site is C5. The order of stability of the adduct species were found to be C6−OH_5Ac• > C4−OH_5Ac• > N3−OH_5Ac• > N5−OH_5Ac• both in the gaseous and solution phase (using the PCM model) respectively due to the additions of •OH at C6, C4, N3, and N5 atoms. These additions occur in direct manner, without the intervention of any precursor complex formation. The possibility of a 1,2-hydrogen shift from the C6 to N5 in the nitrogen-centered C6−OH_5Ac• radical is considered in order to account for the experimental observation of the high yield of non-oxidizing radicals, and found that such a conversion requires activation energy of about 32 kcal/mol, and hence this possibility is ruled out. The hydrogen abstraction reactions were assumed to occur from precursor complexes (hydrogen bonded complexes represented as S1, S2, S3, and S4) resulted from the electrostatic interactions of the lone pairs on the N3, N5, and O8 atoms with the incoming •OH radical. It was found that the conversion of these precursor complexes to their respective transition states has ample barrier heights, and it persists even when the effect of solvent is considered. It was also found that the formation of precursor complexes itself is highly endergonic in solution phase. Hence, the abstraction reactions will not occur in the present case. Finally, the time dependent density functional theory (TDDFT) calculations predicted an absorption maximum of 292 nm for the N3−OH_5Ac• adduct, which is close to the experimentally observed spectral maxima at 290 nm. Hence, it is assumed that the addition to the most reactive center N3, which results the N3−OH_5Ac• radical, occurs via a kinetically driven process.

Introduction

Azapurines and azapyrimidines are structural analogues of purines and pyrimidines. Development of such structural analogues of nucleic acid components and understanding of their antimetabolic activities are important to block the growth of cancer cells. Among the aza analogues, 5-azacytidine was reported to be clinically very promising due to its cytotoxic, antimicrobial, antineoplastic, abortive and mutagenic properties.[1−6] Consequently, the free radical chemistry of the aza compounds is of great importance as tumor treatment involves the simultaneous use of both chemo and radiotherapy.[7] Though these compounds are very relevant in cancer therapy, their free radical chemistry remains poorly understood. An earlier study[2] reported that radiolytically generated water derived free radicals such as hydroxyl radicals (•OH) and hydrated electrons (e_{aq}^-) react with aza analogues of pyrimidine at diffusion-controlled rate (10^9−10^{10} $dm^3\ mol^{-1}\ s^{-1}$) at pH 8, and this order is well comparable to the rates with pyrimidines.[9] However, no details on the reaction mechanism or on the intermediates were reported. Considering the biological importance, 5-azacytosine and its nucleoside, 5-azacytidine, were selected for the study of the reactions of hydroxyl radicals (•OH), which is the most important DNA damaging radical. In addition to their biological importance, a number of interesting radical reactions are expected from these compounds. Hydroxyl radical mainly undergoes addition reactions with cytosine, thymine, and uracil; however a small amount (10%) of hydrogen abstraction is also reported in the case of thymine.[8,9] The major sites of attack of •OH for addition reactions in pyrimidines were identified as C5 and C6 positions.[8,9] In addition to this, an interesting dehydration reaction of the initially formed reducing •OH-adduct radical to an oxidizing radical at the basic medium, is reported in the case of cytosine[9] as well as a number of pyrimidines.[10] All these reactions may be interestingly different in the case of azacytosines due to the presence of nitrogen in the C5 position. Therefore, a detailed investigation of the reaction of •OH with

* Corresponding author. E-mail: (C.T.A.) CT-Aravindakumar@rocketmail.com; (C.H.S.) sureshch@gmail.com

[†] School of Chemical Sciences, Mahatma Gandhi University.

[‡] Radiation Chemistry and Chemical Dynamics Division, Bhabha Atomic Research Centre.

[§] Computational Modeling and Simulation Section, Regional Research Laboratory (CSIR).

10.1021/jp063958a CCC: $33.50
Published on Web 09/21/2006

5-azacytosine and 5-azacytidine is carried out in aqueous medium using pulse radiolysis technique, which is an ideal tool for the study of transient intermediates in solution state. To get a clear picture on the various reaction probabilities as well as to support the experimental interpretations, extensive theoretical calculations were carried out using the Gaussian program.

Experimental Section

Commercially available 5-azacytosine, 5-azacytidine, and 2,2′-azinobis(3-ethylbenzothiazoline-6-sulfonate) ($ABTS^{2-}$), were purchased from Aldrich and were used without further purification. All solutions were prepared in water purified by Millipore Milli-Q system. The concentration of the substrate was kept at 1×10^{-3} mol dm^{-3}. Radiolysis of water produces the highly reactive hydrated electron (e^-_{aq}), hydrogen atom ($H^\bullet$) and hydroxyl radical ($^\bullet OH$) in addition to the formation of inert or less reactive molecular products such as H_2 and H_2O_2.[11]

$$H_2O \rightsquigarrow e^-_{aq}, H^\bullet, {}^\bullet OH, H_2, H_2O_2, H_3O^+ \qquad (1)$$

The reaction of $^\bullet OH$ was carried out in N_2O saturated solutions where e^-_{aq} is quantitatively converted to $^\bullet OH$ (reaction 2).[11]

$$N_2O + e^-_{aq} \rightarrow {}^\bullet OH + OH^- + N_2 \qquad (2)$$

Pulse radiolysis experiments were carried out using a linear accelerator delivering electron pulses of 7 MeV energy of 50 ns duration. An aerated aqueous solution of KSCN (1×10^{-2} mol dm^{-3}) was used to monitor the dose per pulse with $G \times \epsilon_{500} = 21\,520$ dm^3 mol^{-1} cm^{-1} and was normally kept at 10−12 Gy. A low dose per pulse of 6.5 Gy was used for the investigation of the electron-transfer reaction between the transient intermediates and $ABTS^{2-}$. The transient species formed on pulse radiolysis were monitored by using a 450 W pulsed xenon lamp, a monochromator (Kratos GM-252), and a Hamamatsu R-955 photomultiplier as the detector. The photomultiplier output was digitized with a 100 MHz storage oscilloscope interfaced to a computer for kinetic analysis. The details of the pulse radiolysis setup have been described elsewhere.[12]

Computational Method. Density functional theory calculations were performed with Gaussian 03 program.[13] The Becke's three parameter hybrid functional using the correlation functional of Lee, Yang, and Parr (B3LYP)[14] has been proven to be effective for determining the optimal geometries, harmonic frequencies, and electronic properties[15,16] of nucleic acid bases, and it was selected for the current study for the same reason. The geometries were completely optimized without any symmetry constrains. Spin unrestricted calculations were performed for open shell systems. The 6-31+G(d,p) basis set is selected for all calculations, which includes the necessary diffuse and polarization functions for modeling radical systems. Optimized structures were characterized by harmonic vibrational frequencies as local minima (all real frequencies) and saddle points (one imaginary frequency). The transition state geometries were obtained using the QST3 search method.[17] The gas-phase geometries were reoptimized including the effect of aqueous environment using the polarizable continuum model (PCM)[18] implemented in Gaussian 03. Excited-state energies were calculated using the TDDFT method [19] with the same basis set.

Results and Discussion

I. Pulse Radiolysis Study. The second-order rate constants for the reaction of $^\bullet OH$ with 5-azacytosine (5Ac) and 5-azacytidine (5Acyd) at pH 6 were determined from the rate of buildup of the transients at their respective absorption maximum observed at 290 nm. These values are 5.1×10^9 and 5.2×10^9 dm^3 mol^{-1} s^{-1} respectively for 5Ac and 5Acyd. The reported rate constants [2] were 2.2×10^9 dm^3 mol^{-1} s^{-1} and 2.7×10^9 dm^3 mol^{-1} s^{-1} and the present values are slightly higher, however, found to be highly reproducible. The transient absorption spectrum of the reaction of $^\bullet OH$ with 5-azacytosine at 4 μs after the pulse is characterized by its maximum at 290 nm at pH 6 (Figure 1). The time-resolved spectra did not show any significant change with respect to time, in the absorption properties of the transients except a second order decay. Nearly similar spectral properties were obtained at pH 10 as well which is also shown in Figure 1.

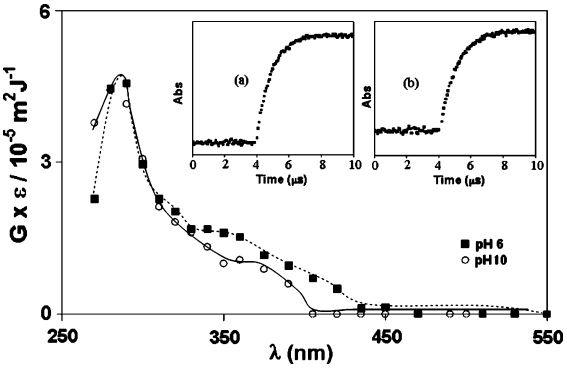

Figure 1. Transient absorption spectrum obtained in N_2O saturated aqueous solutions of 5Ac (1×10^{-3} mol dm^{-3}) at 4 μs after the pulse at pH 6 (■) and at pH 10 (○). Inset: Absorption buildup of $ABTS^{\bullet-}$ at 435 nm obtained from the reaction of the intermediate with $ABTS^{2-}$ (a) at pH 6 and (b) at pH 10.

One of the easiest methods to understand the redox nature of the transient intermediates, is the use of known oxidants/reductants at sufficiently low concentrations so that there will not be any direct reaction of $^\bullet OH$ with the oxidants/reductants, while the intermediates would react with the oxidants/reductants, making use of their slight differences in the oxidation/reduction potentials.[8] To look at the oxidizing nature of the intermediate, low concentration of 2,2′-azinobis(3-ethylbenzothiazoline-6-sulfonate) ($ABTS^{2-}$, 1×10^{-5} mol dm^{-3}) was used to avoid any direct reaction of $^\bullet OH$, and the formation of $ABTS^{\bullet-}$ was monitored at 435 nm at pH 6 and at 10. A very clear absorption buildup of $ABTS^{\bullet-}$ confirmed the presence of an oxidizing intermediate at both the pH (Figure 1). The one electron oxidation of $ABTS^{2-}$ by oxidizing radical intermediates and the corresponding buildup of $ABTS^{\bullet-}$ have been reported earlier.[8]

The yield of $ABTS^{\bullet-}$ was calculated in terms of its G value [20], $G(ABTS^{\bullet-})$ and is 1.5×10^{-7} mol J^{-1} at pH 6, which constitutes only about 27% of the total $^\bullet OH$ reaction.[21] Similarly, $G(ABTS^{\bullet-})$ of 1.3×10^{-7} mol J^{-1} was obtained at pH 10, which constitutes about 23% of the total $^\bullet OH$ reaction. The second-order rate constants of the reaction of the intermediate with $ABTS^{2-}$ at pH 6 and 10 were estimated as 7×10^9 dm^3 mol^{-1} s^{-1} and 5.6×10^9 dm^3 mol^{-1} s^{-1}, respectively. These values are well comparable to the generally observed electron-transfer reaction of the oxidizing intermediates with $ABTS^{2-}$.[22]

The transient absorption spectra obtained from the reaction of $^\bullet OH$ with 5-azacytidine recorded at pH 6 and at pH 10, were characterized by their single maximum at 290 nm (Figure 2). The buildup of $ABTS^{\bullet-}$ was also monitored at 435 nm and the corresponding $G(ABTS^{\bullet-})$ values were 0.6×10^{-7} and $0.4 \times$

SCHEME 1: Possible Addition Reactions of Hydroxyl Radicals with 5-Azacytosines

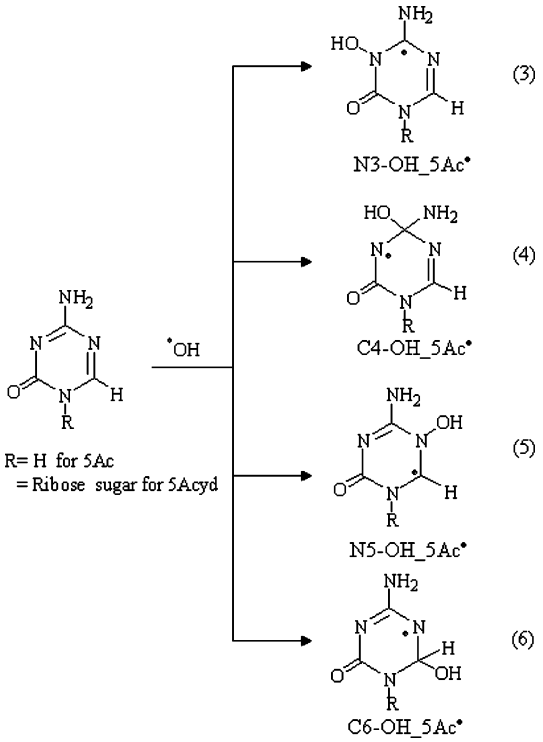

10^{-7} mol J^{-1} at pH 6 and at pH 10, respectively. These values are estimated as 11% and 8%, respectively, of the total •OH reactions.

The nature of the transient intermediate spectra themselves is very different from that obtained for cytosine and cytidine. The transient absorption spectrum from Cyt is characterized by an absorption maximum at 345 nm at pH 6.5, where as the spectral maximum in the case of 5Ac is at 290 nm.[9] More importantly, the redox nature of the intermediates in the present case is widely different from cytosine at higher pH. Assuming an addition reaction, similar to cytosine,[9] one can consider a number of carbon and nitrogen positions feasible for addition for the reaction of •OH with 5Ac and 5Acyd. These probable sites are N3, C4, N5, and C6 (Scheme 1). The addition at nitrogens N3 and N5 would result radicals of the form N3−OH_5Ac • and N5−OH_5Ac• (reactions 3 and 4, Scheme 1), where as the additions at carbons C4 and C6 results radicals of the form C4−OH_5Ac • and C6−OH_5Ac• (reactions 5 and 6, Scheme 1). The radicals resulting from the addition at carbons (C4−OH_5Ac• and C6−OH_5Ac•) could be efficient electron acceptors from reductants such as $ABTS^{2-}$ due to the unpaired spin density at nitrogen or oxygen. Both these radicals can undergo electron-transfer reaction with $ABTS^{2-}$ (reactions 7 and 8) as shown in Scheme 2. It is however difficult to distinguish between these two radicals using $ABTS^{2-}$ as both are oxidizing in nature. The calculated second-order rate constants for the reaction of oxidizing intermediates with $ABTS^{2-}$ are 7×10^9 dm^3 mol^{-1} s^{-1} in the case of 5Ac and 1.4×10^{10} dm^3 mol^{-1} s^{-1} in the case of 5Acyd. These values are nearly similar to the second-order rate constant obtained for the reaction of oxidizing C6−OH_Cyt• radical of cytosine with the well-known reductant, *N*,*N*,*N*′,*N*′-tetramethyl-*p*-phenylenediamine (TMPD) at the same pH.[3,4] On the other hand, the radicals resulting from the addition at nitrogens (N3−OH_5Ac• and N5−OH_5Ac•) will not possess the property of accepting an electron from $ABTS^{2-}$ since the unpaired spin density will be at carbon. It is clear

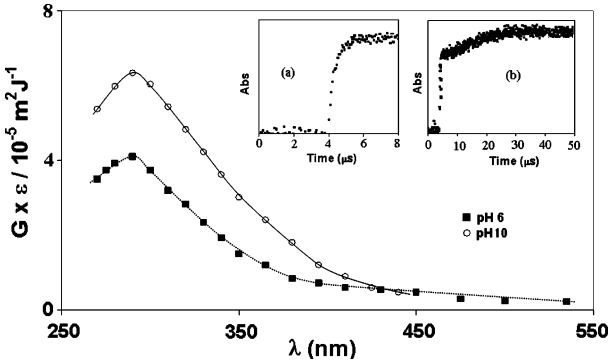

Figure 2. Transient absorption spectrum obtained at 4 μs after the pulse from the pulse radiolysis of 5-azacytidine solutions (10^{-3} mol dm^{-3}) saturated with N_2O at pH 6 (■) and at pH 10 (○). Inset: $ABTS^{\bullet-}$ buildup at 435 nm obtained from the reaction of the intermediate with $ABTS^{2-}$ (a) at pH 6 and (b) at pH 10.

SCHEME 2: Electron Transfer Reactions of C4−OH_5Ac• and C6−OH_5Ac• with $ABTS^{2-}$

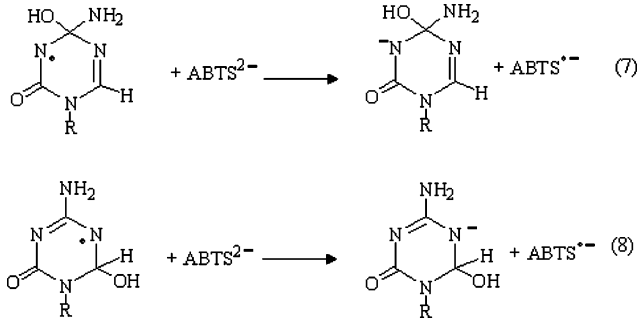

from the yield of $ABTS^{\bullet-}$ that only about 27% from 5Ac and about 11% from 5Acyd, are oxidizing in nature with respect to $ABTS^{2-}$ at pH 6. This leads to the assumption that at pH 6, about 27% of the •OH adducts are the result of addition at carbon (either C4 or C6) and the remaining 73% of the •OH adducts are the result of addition at nitrogen (N3 or N5) in the case of 5Ac.

A low percentage of oxidizing radicals (23% and 8% respectively, for 5Ac and 5Acyd) is obtained at pH 10 also, indicating that a high percentage of non-oxidizing radicals (77% and 92% respectively for 5Ac and 5Acyd) is formed even at higher pH. It is evident from the very similar spectral nature of the intermediate from 5Ac at pH 6 and 10, that similar •OH adducts exists at both the pH. The result obtained at pH 10 differs very much from the reaction of •OH with Cyt at the same pH. The base-catalyzed dehydration reaction of the reducing C5−OH_Cyt• radical to an oxidizing radical at higher pH[3] is absent in the present case with 5Ac. Both the spectral characteristics and the yield of $ABTS^{\bullet-}$ are nearly the same at pH 10 compared to those at pH 6 (Figure 1).

The spectral behavior from 5Acyd at pH 6 and pH 10 is very similar except that the G×e is slightly higher at pH 10 [$\Delta(G \times \varepsilon) = 2.24$] (Figure 2). This higher value is likely due to the deprotonation of the OH adduct radical. The transient absorption spectrum (Figure 2) is, therefore, attributed to the existence of the non-oxidizing OH adducts radicals. The buildup of absorbance of $ABTS^{\bullet-}$ at pH 10 has a slightly different nature compared to that of 5Ac (Figure 2). The initial buildup of absorbance was complete in about 5 μs and then it undergoes a slow build up. As can be seen from Figure 2 that the absorbance reaches a plateau value after about 40 μs. However, only about 2% increase in the G value was calculated for this later build up (i.e., the difference in the G values after the initial

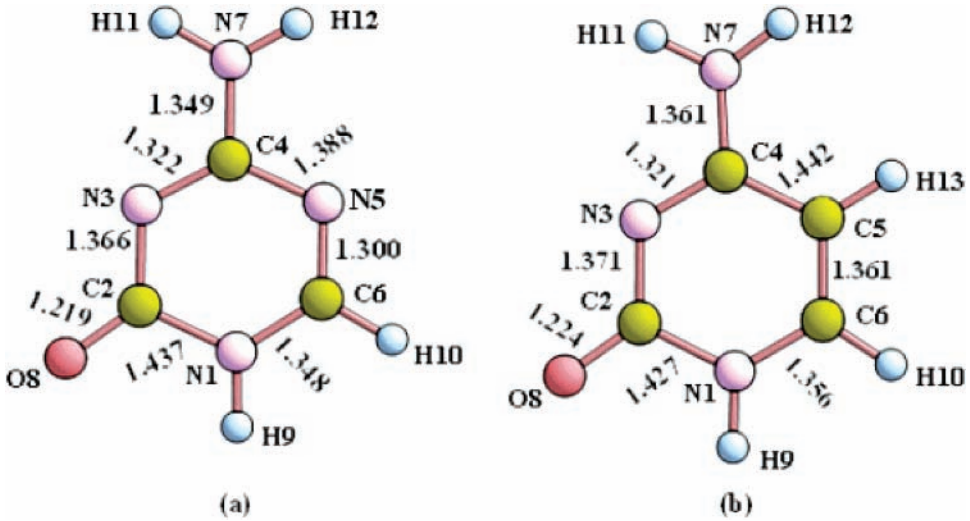

Figure 3. Optimized geometry of 5Ac and Cyt at the B3LYP/6-31+G(d,p) level of theory. Bond lengths are in Å units.

fast build up and the later slow build up). This phenomenon indicates that a minor fraction of the initially formed reducing radicals get converted to oxidizing radicals in basic medium, as observed in the case of cytosine and some of its derivatives.[3,10] However, there is a significant difference in the yield of the oxidizing radicals in neutral and basic pH in the case of cytosine and its derivatives. Since this difference is very marginal in the present case, such a change in the redox behavior is not highlighted.

Although the experimental results resolve the existence of radicals from addition at nitrogen and at carbon centers, it is rather difficult to clearly identify the exact structures of the OH adduct radicals. To shed some light on the various reaction probabilities (some of those probabilities were not considered in the interpretation of the experimental results), we have carried out a detailed DFT calculations and the results obtained from these calculations are now discussed.

II. Theoretical Study. *(a) Structure and Electronic Properties of 5-Azacytosine.* The optimized geometry of 5-azacytosine at B3LYP/6-31+G(d,p) level of theory in a vacuum is depicted in Figure 3a along with the important bond length parameters. For a comparison of the geometry, the isoelectronic natural base cytosine is also optimized at the same level of theory (Figure 3b). The dihedral angle τ(H11−N7−C4−N5) is 180.0° for 5Ac, suggesting a planar geometry, whereas the corresponding H11−N7−C4−C5 dihedral angle for Cyt is 174.7°, suggesting a slight pyramidalization of the amino group. We can see that the shortest bond found in the ring is between N5 and C6 for 5Ac (1.300 Å), and C5 and C6 (1.361 Å) for Cyt. The N3C4 bond of length 1.322 and 1.321 Å, respectively, for 5Ac and Cyt is also largely localized as a double bond. The bond between the amino nitrogen N7 and C4 is significantly shorter than a typical CN single bond (1.472−1.479 Å) for both systems, which may be attributed to the strong resonance interaction between the nitrogen lone pair and the ring π-system. However, the C4N7 bond in 5Ac, of length 1.349 Å, is 0.012 Å shorter than that of cytosine. This suggests that 5-azacytosine has a stronger resonance interaction between the nitrogen lone pair and the ring π-system as compared to cytosine which is also supported by the more planar character of the amino group in 5Ac. The above-mentioned structural features of cytosine and 5Ac are found to be in good agreement with the MP2/6-31G(d,p) level study on these systems reported by Yevgeniy et al.[23]

Since more double bond character is found in N3C4 and N5C6(or C5C6 in Cyt) bonds, the constituent atoms of these bonds are expected to be more reactive than the rest for an electrophilic addition reaction with hydroxyl radical. To gain additional information regarding the electron rich centers, the molecular electrostatic potential (MESP)[24,25] of both systems were analyzed at B3LYP/6-31+G(d,p) level of theory. The MESP plotted on the van der Waals' surface is given in Figure 4, parts a and b, for 5Ac and Cyt, respectively, suggests quite similar electron distribution at the π-face of both the systems. The π-faces of both the systems are more electron rich around the region showing maximum double bond character than the N1C6 region (red region with more single bond character) and this feature is more dominant in the 5Ac molecule. A more quantitative picture regarding the lone pair strength of N and O atoms is also obtained by locating the most negative valued MESP point (V_{min})[24,25] in these systems. In the case of 5Ac, the V_{min} points are located near the O8, N3, and N5 atoms (Figure 4c) while in the case of Cyt these values are located near O8 and N3 atoms (Figure 4d).

(b) Reactivity of 5Ac toward Hydroxyl Radical: Formation of 5Ac...•OH Hydrogen-Bonded Complexes. Among the reactive oxygen species, hydroxyl radicals modify the DNA bases either by addition or hydrogen abstraction reactions.[8] In the present case, we have considered these two reaction possibilities synchronously only for 5Ac, since an elaborate theoretical study of the reaction of hydroxyl radical with cytosine was already reported by Ji et al.[26] The structural features of 5Ac favor N3, C4, N5, and C6 as the addition sites. There are four abstractable hydrogen atoms viz. the H9 attached to the N1 atom, the H10 attached to the C6 atom, and the H11 and H12 attached to N7.

At first we have considered the possibility of the formation of a π-complex. Two situations were considered, one in which the hydrogen of •OH pointed toward the π-face, and the other in which the oxygen of •OH is pointed toward the π-face. In both the cases, the •OH radical moved out from the π-face to the molecular plane and eventually led to the formation of hydrogen bonded (H-bonded) complex **S1** as depicted in Figure 5. In this complex, the H of •OH form an H-bond with the carbonyl oxygen at a distance of 1.781 Å, while oxygen •OH is in an H-bond with H9 at a distance of 2.071 Å. As the H-bonded complex formation is mainly aroused from the electrostatic interaction of •OH radical and the lone pair on the carbonyl oxygen, the interactions of the lone pairs on the N3, and N5 atoms (see the MESP plot in Figure 4c) with the hydrogen of •OH radical can also lead to the formation of H−bond

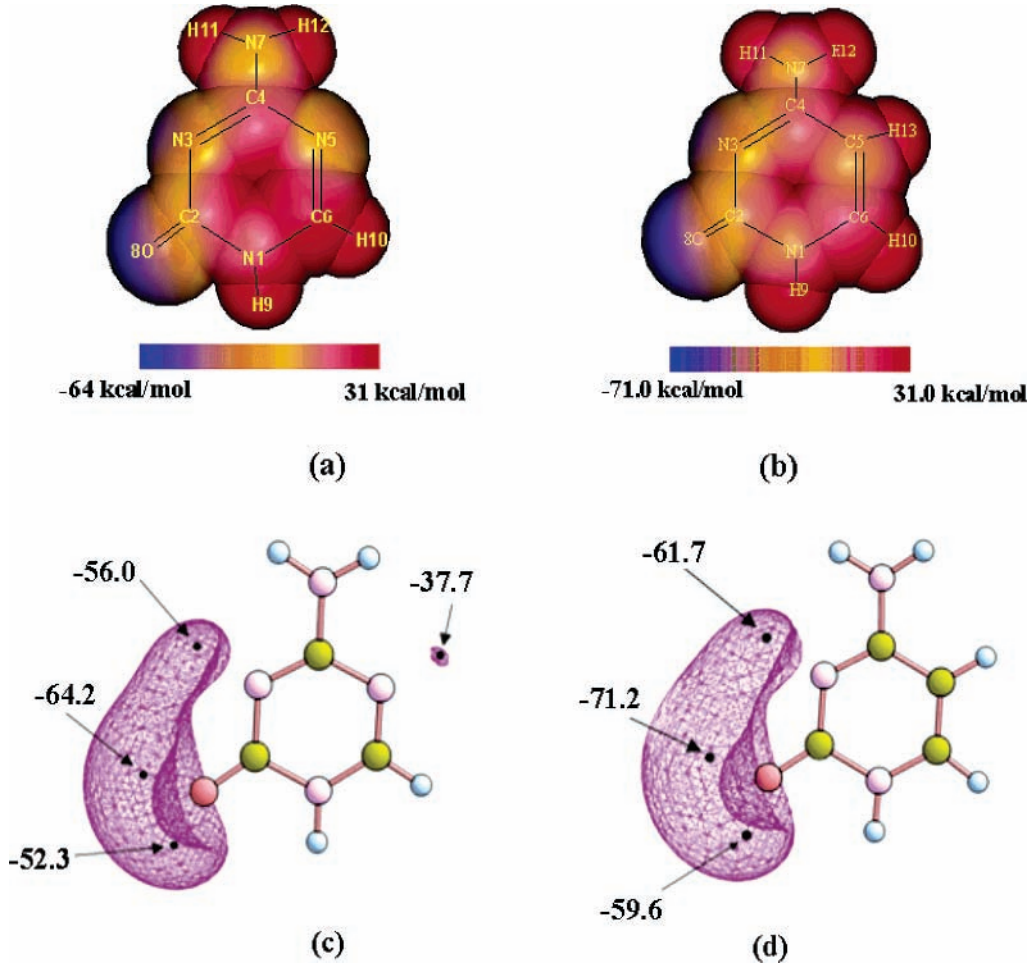

Figure 4. The electronic features of 5Ac and Cyt. Key: (a and b) MESP plotted on the van der Waals surface; (c and d) V_{min} points located near the O8, N3, and N5 atoms. An isosurface of value −35.75 kcal/mol is also depicted.

complexes **S2**, **S3**, and **S4**. The optimized geometries of these systems are also shown in Figure 5.

The BSSE-corrected interaction energies (i.e., binding energy of •OH) of the H-bonded complexes are also depicted in Figure 5. The strength of the interaction is in the order **S3** > **S4** > **S1** > **S2**.

(c) Addition Reactions. As we have seen that the formation of a π-complex is an unlikely process, the adduct formation reactions is expected to be a spontaneous reaction leading to the direct addition of hydroxyl radical to the 5Ac system. An inspection of the HOMO (Figure 6) of 5Ac suggests that the most dominant site for an electrophilic addition of •OH radical is the N3 atom of the N3C4 double bond as it shows the highest orbital coefficient. Also depicted in Figure 6 is the HOMO of Cyt, wherein the C5 atom of the C5C6 double bond has the largest MO coefficient. In fact, the Cyt is known for its addition reaction with •OH at the C5 atom giving rise to the C6-centered radical.[9]

Although, N3 atom is expected to be the most reactive, we have considered the possibility of the addition of •OH with the constituent atoms of the double bonds, viz. N3, C4, N5, and C6. Therefore, reactions 3−6 (see Scheme 1) yielding the radical systems N3−OH_5Ac•, C4−OH_5Ac•, N5−OH_5Ac•, and C6−OH_5Ac• have been modeled. The optimized geometries of these radical systems are depicted in Figure 7 along with their relative energy values with respect to the sum of the energies of 5Ac and •OH. For the •OH addition products N3−OH_5Ac• and N5−OH_5Ac•, the spin maximum is centered on C6 atom, and these values, respectively, are 0.70 and 0.78, suggesting higher delocalization of the unpaired electron in the former radical. However for the C4−OH_5Ac• adduct, the spin density value is at a maximum on the N3 (0.74) atom, and for the C6−OH_5Ac• adduct, the spin maxima were found on the N3 (0.45) and N5 (0.63) atoms.

According to the relative energy values, the order of stability of adduct systems are C6−OH_5Ac• > C4−OH_5Ac• > N3−OH_5Ac• > N5−OH_5Ac•. The relative enthalpies as well as the relative free energy values of these radical systems also show the same trend as that of relative energy values (Figure 8). The formation of the N3−OH_5Ac• and the N5−OH_5Ac• radicals are 9.24 and 18.65 kcal/mol endothermic, where as the formation of the C4−OH_5Ac• and the C6−OH_5Ac• adducts are exothermic by 1.13 and 13.01 kcal/mol, respectively. Therefore, the observed N-centered radical system in the experiment can be considered as C6−OH_5Ac• while the C-centered radical system in the experiment may be N3−OH_5Ac•. However, it may be noted that the amount of C-centered radical (73%) formed in the experiment was much higher than the amount of N-centered radical (27%), which cannot be explained by the thermodynamic stability of the adducts alone. Since the reactivity of the HOMO orbital is in favor of the addition of •OH radical at the N3 atom leading to the formation of the C-centered radical N3−OH_5Ac•, we can assume that a higher yield of this product observed in the experiment is due to the kinetic control of the reaction.

It may be noted that the calculated stability order of the different adduct systems of cytosine obtained by Ji et al.[26] follows the order C6−OH_Cyt• > C5−OH_Cyt• > C4−

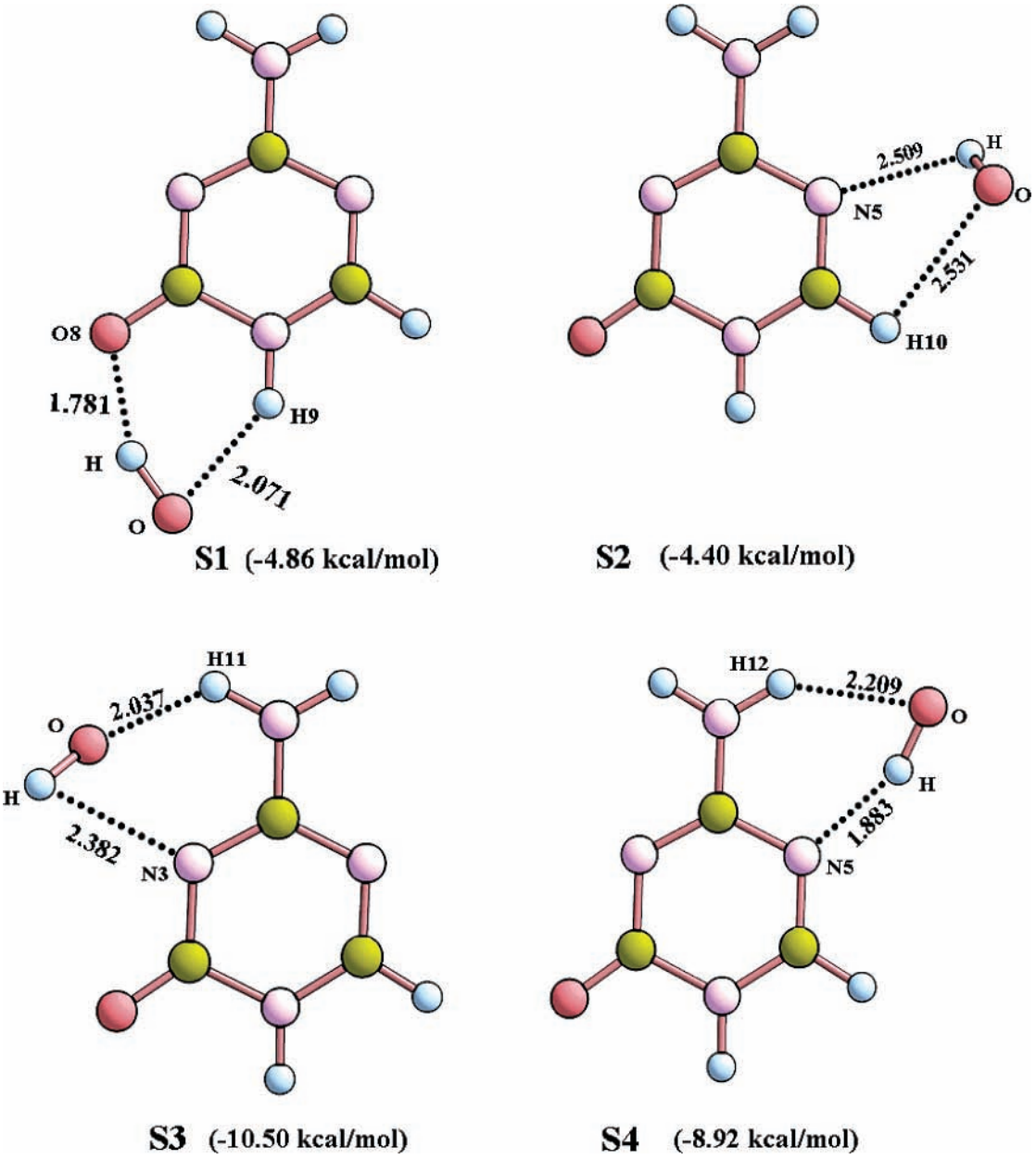

Figure 5. B3LYP/6-31+G(d,p) level optimized geometry of the H-bonded complexes. BSSE corrected interaction energy is shown in parentheses.

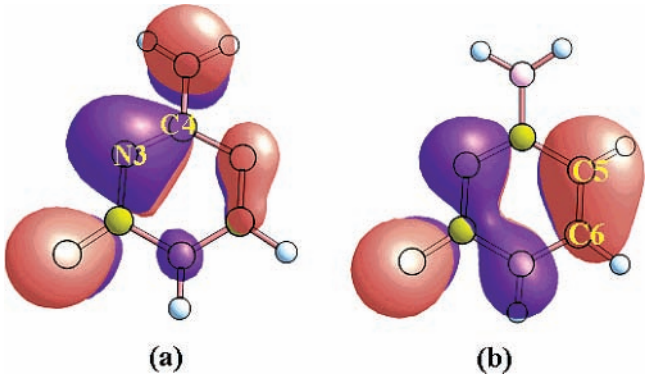

Figure 6. Highest occupied molecular orbital of (a) 5Ac and (b) Cyt.

OH_Cyt$^\bullet$ > N3−OH_Cyt$^\bullet$. Their result suggested that the formation of the experimentally observed product C5−OH_Cyt$^\bullet$ was mainly a kinetically controlled process.

(d) 1,2-Hydrogen Shift. The formation of a reducing radical (C-centered) is derived in a kinetically driven process as we have seen above; an alternate possibility for the formation of a C-centered radical is considered by the 1,2-hydrogen migration from C6 to N5 of the initially formed C6−OH_5Ac$^\bullet$ adduct (N-centered radical) leading to the isomeric C6−OH_N5H_5Ac$^\bullet$ radical (a C-centered radical). This possibility is considered because the energetics of addition reactions discussed in the previous section suggested a high stability for C6−OH_5Ac$^\bullet$. The hydrogen transfer can be envisaged to occur from C6 to N5 via the transition state **TS1**.

The geometrical features of the optimized structures are shown in Scheme 3. In **TS1**, the labile hydrogen atom is acting as a bridge between N5 and C6 atoms. The calculated activation energy for this transformation is 32.0 kcal/mol and the product system showed a 8.06 kcal/mol higher stability than the reactant at B3LYP/6-31+G(d,p) level of theory. Although the reaction is exothermic, the activation barrier is considerably above the reaction enthalpies of a feasible reaction, and it seems safe to assume that such a process may not occur at the conditions used in the experiment. We have also computed the activation energy

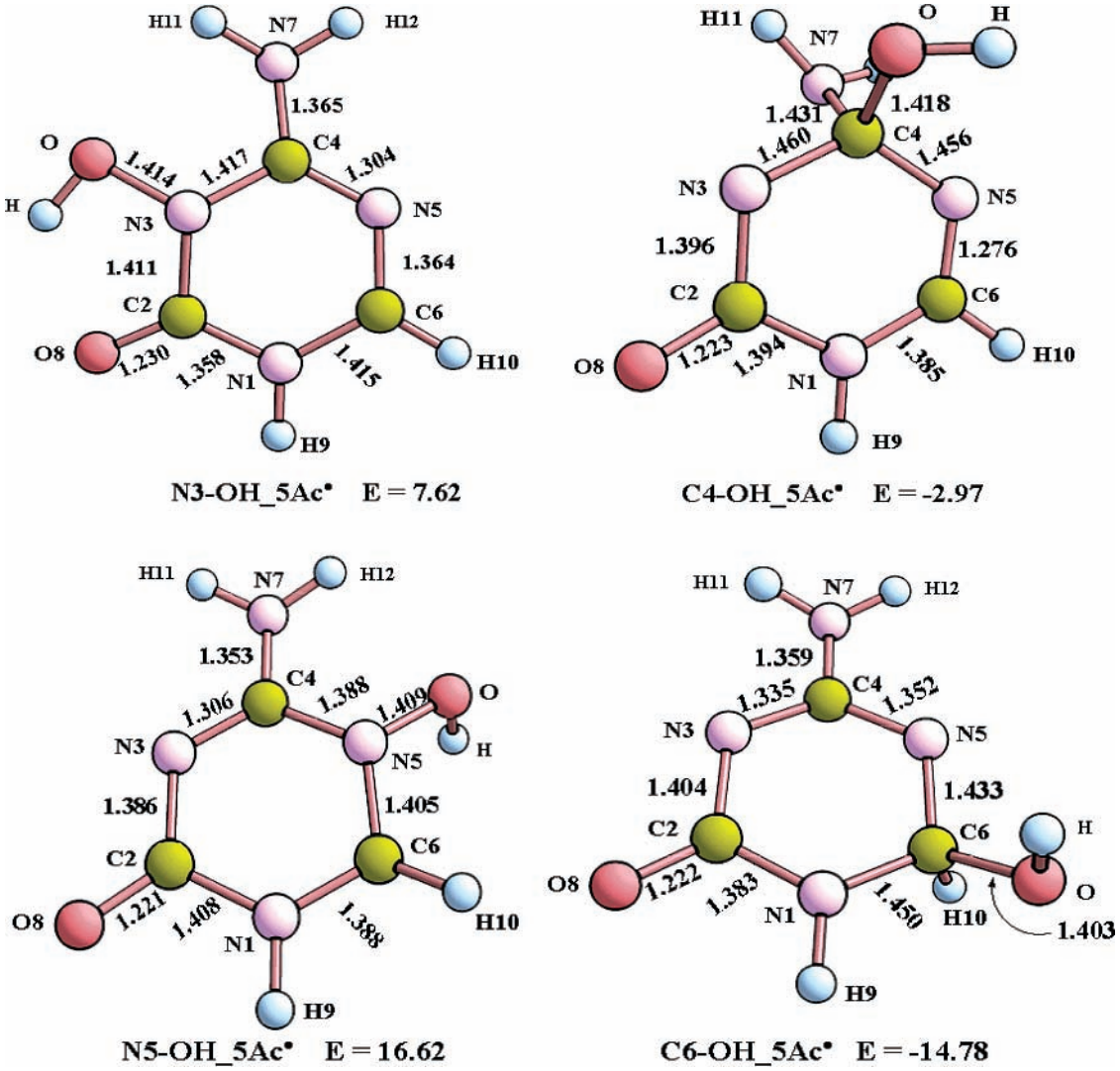

Figure 7. Optimized structures of possible •OH adducts of 5Ac. The relative energy values (*E*) in kcal/mol are also given. All bond lengths in Å.

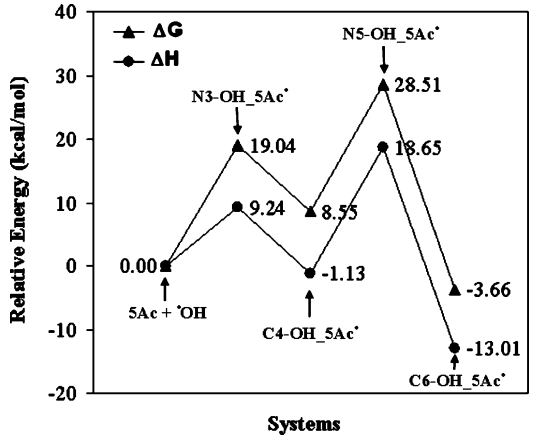

Figure 8. Relative enthalpy change (Δ*H*) and free energy change (Δ*G*) for the OH addition reactions computed at the B3LYP/6-31+G(d,p) level of theory.

at the MP2/6-31+G(d,p) level of theory, and the result turned out to 31.6 kcal/mol.

(e) Hydrogen Abstraction Reactions. In this section we have considered the possibility of the formation of N-centered and C-centered radical systems resulting from hydrogen abstraction reactions. It is already seen that •OH radicals can form H-bonded complexes with 5Ac and hydrogen abstraction reactions may

SCHEME 3: 1,2-Hydrogen Transfer from C6 to N5 in C6−OH_5Ac• Adduct[a]

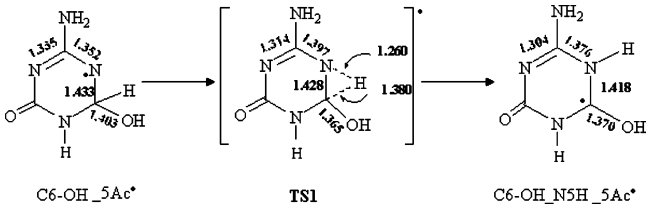

[a] Bond lengths are in Å.

occur from these complexes. The transition states **TS2**, **TS3**, **TS4**, and **TS5** corresponding to the abstraction of H9 in **S1**, H10 in **S2**, H11 in **S3**, and H12 in **S4** are located and are depicted in Figure 9. In all the **TS**s, the abstractable hydrogen atom is located closer to the •OH group. Further, the product radical systems **P1**, **P2**, **P3**, and **P4**, corresponding to the H9, H10, H11, and H12 abstractions are also determined (see Supporting Information). The spin density values of these radical systems are observed mainly on two atoms, viz. (O8 = 0.57, N5 = 0.32) in **P1**, (C6 = 0.74, N5 = 0.11) in **P2**, (N7 = 0.76, N3 = 0.39) in **P3**, and (N7 = 0.76, N3 = 0.36) in **P4**. It may be noted that except **P1**, all the systems showed the maximum spin density on the atom from which the hydrogen has been abstracted (Figure 9). In the case of **P1**, the spin density

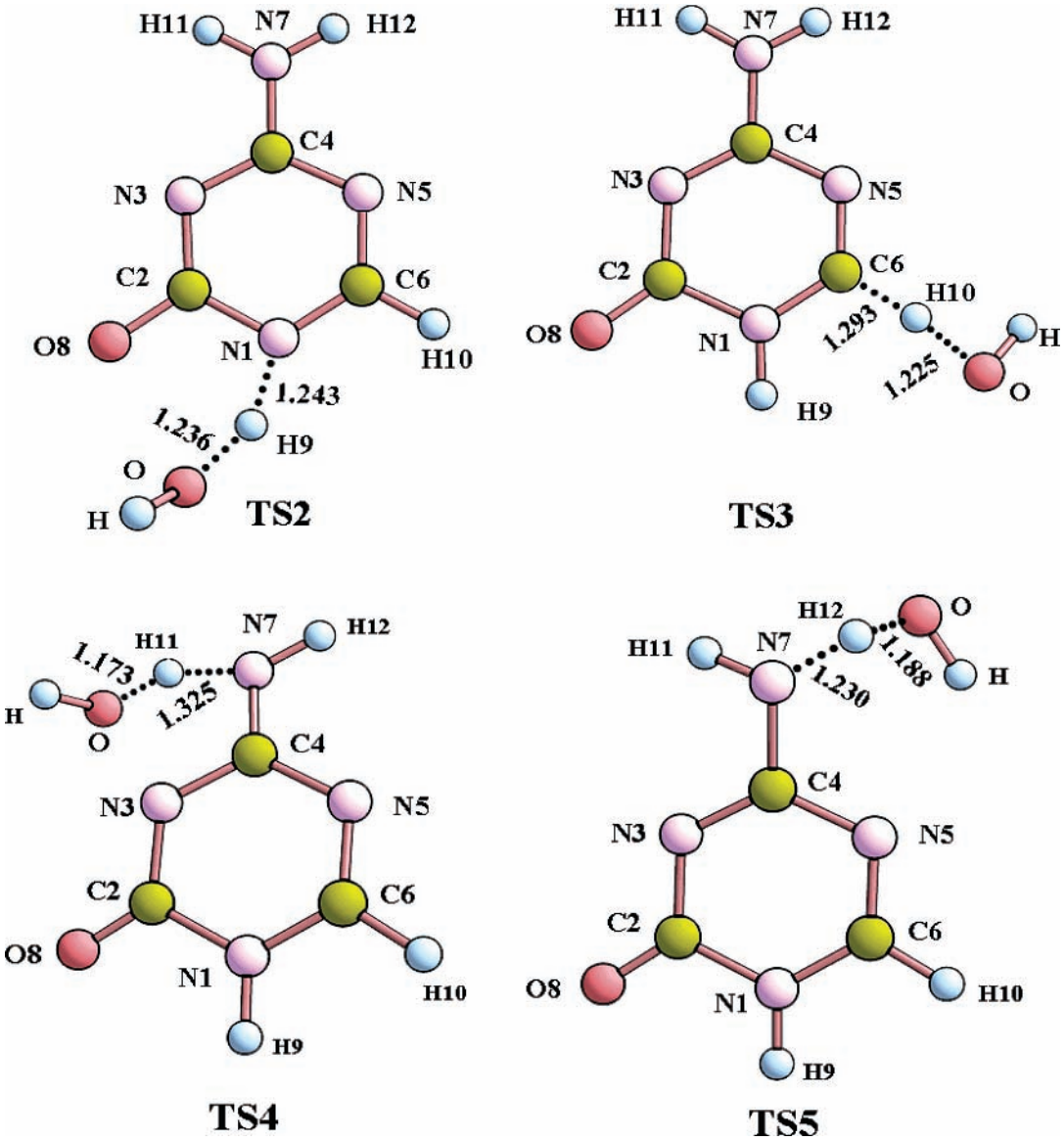

Figure 9. Transition states corresponds to the H abstraction reactions using the QST3 approach at the B3LYP/6-31+G(d,p) level of theory. H-bond lengths are in Å units.

distribution suggests more delocalization of the odd electron as compared to other systems.

The relative enthalpy and free energy changes of reactions (in kcal/mol) [5Ac + •OH] → S_1→ **TS2** → [**P1** + H_2O], [5Ac + •OH] → S_2 → **TS3** → [**P2** + H_2O], [5Ac + •OH] → S_3 → **TS4** → [**P3** + H_2O], and [5Ac + •OH] → S_4 → **TS5** → [**P4** + H_2O] are depicted in Figures 10 and 11, respectively.

It can be seen from the enthalpy profile that all the H-bonded complexes are more stable than the separated system [5Ac + •OH]. Among them the **S3** complex showed the highest stability of 8.24 kcal/mol while the **S2** system showed the least stability of 3.11 kcal/mol. Only in the case of **S2** the hydrogen abstraction was exothermic which led to a more stable system [**P2** + H_2O]. For all the other cases, the hydrogen abstraction reactions from the H-bonded complexes were found to be endothermic. The H-abstractions from **S1** and **S2** were nearly barrierless processes. In the case of **S3** and **S4**, the hydrogen abstraction reactions required activation energies of 9.71 and 8.62 kcal/mol, respectively.

As can be seen from the relative free energy plot that the formation of the H-bonded complexes are endergonic processes, as the entropy of the system decreases on going from separated systems to the associated systems. However, the formations of the product systems are exergonic processes as the entropy for

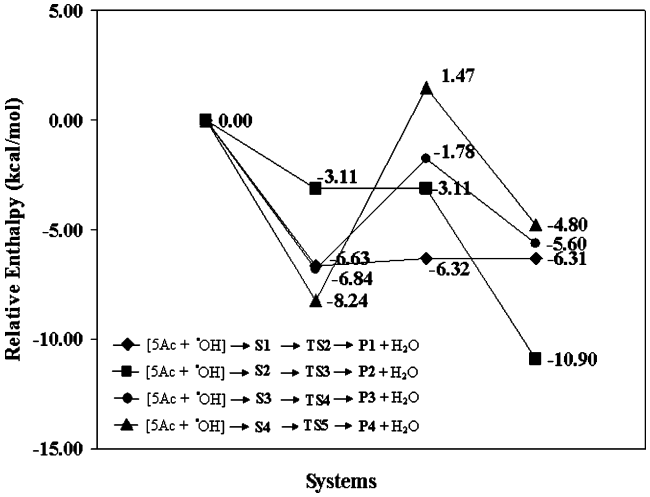

Figure 10. Relative enthalpy profile of the H abstraction reactions computed at the B3LYP/6-31+G(d,p) level of theory

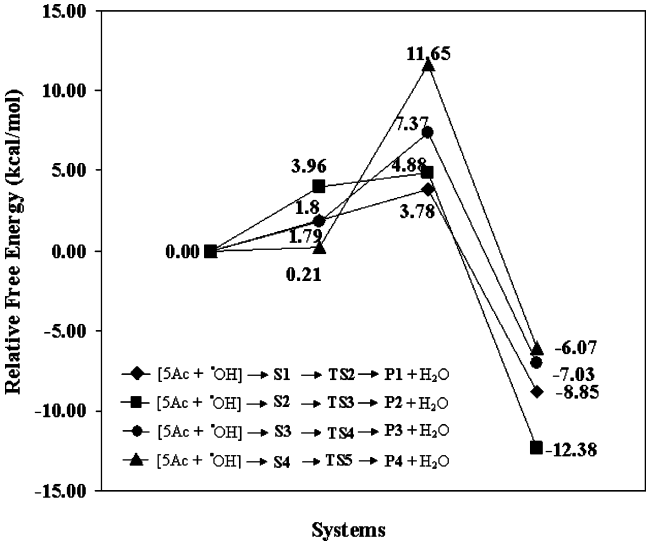

Figure 11. Relative free energy profile of the H abstraction reactions computed at the B3LYP/6-31+G(d,p) level of theory.

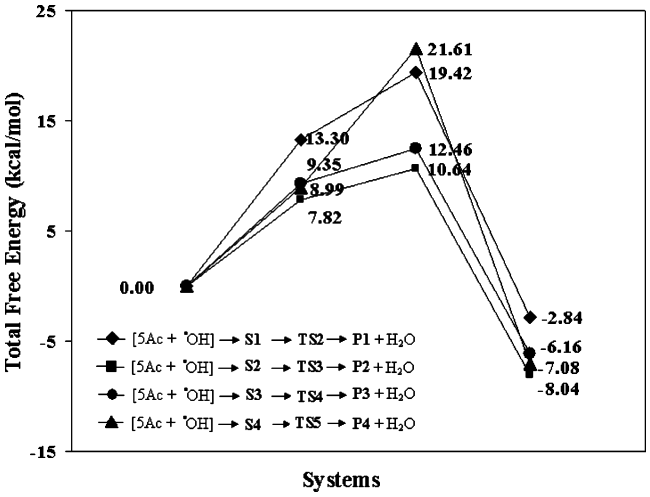

Figure 12. Relative total free energy change (ΔG) for the H abstraction reactions computed at the B3LYP/6-31+G(d,p) level of theory in the solution phase.

these processes are positive. The activation free energy barriers for the formation of the product molecules are 1.99, 0.92, 11.44, and 5.48 kcal/mol respectively for the abstractions of H9, H10, H11, and H12 atoms.

When the effect of solvation is taken into account using the PCM model, it was observed that the solvation considerably influences the relative free energies of the H-bonded complexes and the product molecules as can see in Figure 12. [The total free energy values were calculated by adding the ΔG solvation correction to the gas-phase free energy values.] It can be seen that free energies of the H-bonded complexes increases on comparing with the gas-phase data. The stability of the complexes **S1**, **S2**, **S3**, and **S4** decreases by 15.08, 4.32, 8.79, and 9.71 kcal/mol respectively in the presence of solvent. All theses reactions show activation free energy barrier in the range of 3−12 kcal/mol, which is within the acceptable limit of a facile reaction. However, as the formation H-bonded complexes **S1**, **S2**, **S3**, and **S4** are highly endergonic processes in the solution phase, we can assume that formation of the H-bonded complexes is unlikely to occur in the solution phase, and hence, the hydrogen abstraction reactions may not occur.

(f) TDDFT Calculations. The optical absorption maxima (transition wavelength λ) calculated using the TDDFT method for the C-centered radical species N3−OH_5Ac• is 292 nm in the gas phase. This value is found to be very close to the λ_{max} observed at 290 nm in the pulse radiolysis experiment for a C-centered radical species. On the other hand, the higher intensity transition computed for other transient systems (viz. C6−OH_5Ac• (462 nm), C4−OH_5Ac• (326 nm), and N5−OH_5Ac• (355 nm)) that we have considered did not give a value close to this species. Thus, the TDDFT results support the formation of N3−OH_5Ac• as the most probable C-centered radical system.

Conclusion

The mechanism of the reaction of •OH with 5Ac and 5Acyd is very different from the reaction with Cyt. While •OH undergoes addition at carbon centers (mainly at C5) of Cyt, the major attack of •OH is at the nitrogen (N3) in the case of 5Ac and 5Acyd. The redox reaction of the intermediates from 5Ac and 5Acyd is similar to that from cytosine at near neutral pH while it is very different at higher pH. The interesting transformation of the reducing intermediate radical at neutral pH, to oxidizing radical at higher pH in the case of Cyt is completely absent with 5Ac. Theoretical studies demonstrate that the attack of •OH at N3 in the case of 5Ac is kinetically controlled, though the attack at C6 is energetically more favorable similar to that of Cyt. The addition reactions are assumed to occur in a direct fashion, without the involvement of any precomplex formation. Subsequently, the possibility of hydrogen abstraction reaction of •OH is ruled out. The experimental results are thus fully supported by theoretical calculations.

Acknowledgment. We thank the Board of Research in Nuclear Sciences (BRNS), Mumbai for Financial support. We also thank Prof. B. S. M. Rao and Dr. A. Kumbar at the National Centre for Free Radical Research (NCFRR), Pune, India, for extending pulse radiolysis facility for part of this work.

Supporting Information Available: Tables of Cartesian coordinates, absolute energies, and thermodynamic quantities of the optimized geometries of all the molecules and a figure showing the structures of hydrogen abstracted radicals **P1**, **P2**, **P3**, and **P4**. This material is available free of charge via the Internet at http://pubs.acs.org.

References and Notes

(1) Van-Hoff, D. D.; Slavik, M.; Muggia, C. M. *Am. Intern. Med.* **1976**, *85*, 237.

(2) Rosenthal, P.; Riesz.; Faraggi, M. *Int. J. Radiat. Biol.* **1983**, *44*, 463.

(3) Townsend, A.; Leclerc, J. M.; Dutachman, G.; Cooney, D.; Cheng, Y. C. *Cancer Res.* **1985**, *45*, *8*, 3522.

(4) Maley, I. *Cancer* **1977**, *5*, 327.

(5) Kittler, L.; Hradecna, Z.; Jacob, H. E.; Löber, G. *Z. Allg. Mikrobiole.* **1975**, *15* (5), 323.

(6) (a) Karon, M.; Sieger, L.; Leimbrock, S.; Finklestein, J. Z.; Nesbit, M. E.; Swaney, J. J. *Blood* **1973**, *42*, 359. (b) Rivard, G. E.; Momparler, R. L.; Demers, J.; Benoit, P.; Raymond, R.; Lin, K. T.; Momparler, L. F. *Leukemia Res.* **1981**, *5*, 453. (c) Krooth, R. S.; Hsiao, W. L.; Lam, G. F. M.; *Biochem. Pharmacol.* **1979**, *28*, 1071. (d) Allen, L. B.; Huffman, J. H.; Cook, P. D.; Meyer, Jr., R. B.; Robins, R. K.; Sidwell, R. W. *Antimicrobiol. Ag. Chemother.* **1977**, *12*, 114. (e) Revakar, G. R.; Gupta, P. K.; Adams, A. D.; Dalley, N. K.; McKernan, P. A.; Cook. P. D.; Canonico, P. G.; Robins, R. K. *J. Med. Chem.* **1984**, *27*, 1389.

(7) Liu, M. C.; Luo, M. Z.; Mozdziesz, D. E.; Lin, T. S.; Dutschman, G. E.; Cheng, Y. C.; Sartorelli, A. C. *Nucleosides Nucleotides Nucleic Acids* **1999**, *18*, *1*, 55.

(8) von Sonntag, C. *The Chemical Basis of Radiation Biology*, Taylor and Francis: London, 1987.

(9) (a) Hazra, D. K.; Steenken, S. *J. Am. Chem. Soc.* **1983**, *105*, 4380. (b) Hayon, E.; Simic, M. *J. Am. Chem. Soc.* **1973**, *95*, 1029. (c) Fugita, S.; Steenken, S. *J. Am. Chem. Soc.* **1981**, *103*, 2540. (d) Schuchmann, H.-P.; von Sonntag, C. *Int. J. Radiat. Biol.* **1986**, 49, 1.

(10) Luke, T. L.; Jacob, T. A.; Mohan, H.; Destaillats, H.; Manoj, V. M.; Manoj, P.; Mittal, J. P.; Hoffmann, M. R.; Aravindakumar, C. T. *J. Phys. Org. Chem.* **2002**, *15*, 293.

(11) Steenken, S. *Chem. Rev.* **1989**, *89*, 503.

(12) Aravindakumar, C. T.; Mohan, H.; Mudaliar, M.; Rao, M. B. S.; Mittal, J. P.; Schuchmann, M. N.; von Sonntag, C. *Int. J. Radiat. Biol.* **1994**, *66*, 351.

(13) Gaussian 03, Revision C. 02. Frisch, M. J.; Trucks, G. W.; Schlegel, H. B.; Scuseria, G. E.; Robb, M. A.; Cheeseman, J. R.; Montgomery, Jr., J. A.; Vreven, T.; Kudin, K. N.; Burant, J. C.; Millam, J. M.; Iyengar, S. S.; Tomasi, J.; Barone, V.; Mennucci, B.; Cossi, M.; Scalmani, G.; Rega, N.; Petersson, G. A.; Nakatsuji, H.; Hada, M.; Ehara, M.; Toyota, K.; Fukuda, R.; Hasegawa, J.; Ishida, M.; Nakajima, T.; Honda, Y.; Kitao, O.; Nakai, H.; Klene, M.; Li, X.; Knox, J. E.; Hratchian, H. P.; Cross, J. B.; Adamo, C.; Jaramillo, J.; Gomperts, R.; Stratmann, R. E.; Yazyev, O.; Austin, A. J.; Cammi, R.; Pomelli, C.; Ochterski, J. W.; Ayala, P. Y.; Morokuma, K.; Voth, G. A.; Salvador, P.; Dannenberg, J. J.; Zakrzewski, V. G.; Dapprich, S.; Daniels, A. D.; Strain, M. C.; Farkas, O.; Malick, D. K.; Rabuck, A. D.; Raghavachari, K.; Foresman, J. B.; Ortiz, J. V.; Cui, Q.; Baboul, A. G.; Clifford, S.; Cioslowski, J.; Stefanov, B. B.; Liu, G.; Liashenko, A.; Piskorz, P.; Komaromi, I.; Martin, R. L.; Fox, D. J.; Keith, T.; Al-Laham, M. A.; Peng, C. Y.; Nanayakkara, A.; Challacombe, M.; Gill, P. M. W.; Johnson, B.; Chen, W.; Wong, M. W.; Gonzalez, C.; Pople, J. A. Gaussian, Inc.: Wallingford C T, 2004.

(14) (a) Becke, A. D. *J. Chem. Phys.* **1993**, *98*, 5648. (b) Lee, C.; Yang, W.; Parr, R. G. *Phys. Rev. B* **1988**, *37*, 785.

(15) Santamaria, R.; Charro, E.; Zacarias, A.; Castro, M. *J. Comput. Chem.* **1999**, *20*, 511.

(16) Rastogi, V. K.; Singh, C.; Jain, V.; Palafox, M. A. *J. Raman Spectrosc.* **2000**, *31*, 1005.

(17) (a) Peng, C. Y.; Schlegel, H. B. *Isr. J. Chem.* **1994**, *33*, 449. (b) Peng, C. Y.; Ayala, P. Y.; Schlegel, H. B.; Frisch, M. J. *J. Comput. Chem.* **1996**, *17*, 49.

(18) (a) Tomasi, J.; Persico, M. *Chem. Rev.* **1994**, *94*, 2027.(b) Miertus, S.; Scrocco, E.; Tomasi, J. *Chem. Phys.* **1981**, *55*, 117. (c) Cossi, M.; Scalamni, G.; Rega, N.; Barone, V. *J. Chem. Phys.* **2002**, *117*, 43.

(19) Stratmann, R. E.; Scuseria, G. E.; Frisch, M. J. *J. Chem. Phys.* **1998**, *109*, 8218.

(20) G-value, the number of specified chemical events produced in an irradiated substance per 100 eV of energy absorbed from ionizing radiation. The SI unit is mol J^{-1}. (1 molecule (100 eV)$^{-1}$ = 1.036 × 10^{-7} mol J^{-1}).

(21) The actual yield of $^{\bullet}$OH is calculated as 5. 5 × 10^{-7} mol J^{-1} and hence the G-value calculated for $ABTS^{\bullet-}$ (i.e. 1.5 × 10^{-7} mol J^{-1}) in the present case is equivalent to 27% of the total $^{\bullet}$OH reaction. For more see: Schuler, R. H.; Hartezell, A. L.; Behar, B. *J. Phys. Chem.* **1981**, *85*, 192.

(22) McCord, J. M.; Fridovich, I. *J. Biol. Chem.* **1969**, *244*, 6049.

(23) Yevgeniy, P.; Yury, V. R.; Jerzy, L. *J. Phys. Chem. A* **2000**, *104*, 9964.

(24) The MESP of a molecule is a real physical property and that can be determined experimentally by X-ray diffraction techniques or calculated rigorously from its electron density $\rho(\mathbf{r})$ distribution by employing the equation,

$$V(r) = \sum_{A}^{N} \frac{Z_A}{|r - R_A|} - \int \frac{\rho(r')\, d^3r'}{|r - r'|}$$

where Z_A is the charge on nucleus A, located at $\mathbf{R}_A$. Since MESP is directly related with the electron density distribution, the local minima of MESP (the most negative-valued MESP) is often observed at the electron rich regions such as lone pair and π-bonded regions of a molecule.

(25) For more on MESP, see: (a) Politzer, P.; Truhlar, D. G. *Chemical Applications of Atomic and Molecular Electrostatic Potentials*; Plenum: New York, 1981. (b) Gadre, S. R.; Shirsat, R. N. *Electrostatics of Atoms and Molecules*; Universities Press: Hyderabad, India, 2000. (c) Suresh, C. H.; Gadre, S. R. *J. Org. Chem.* **1999**, *64*, 2505. (d) Suresh, C. H.; Gadre, S. R. *J. Am. Chem. Soc.* **1998**, *120*, 7049. (e) Suresh, C. H.; Koga, N. *Inorg. Chem.* **2002**, *41*, 1573.

(26) Ji, Y. J.; Xia, Y. Y.; Zhao, M. W.; Huang, B. D.; Li, F. *J. Mol. Struct.: THEOCHEM* **2005**, *723*, 123.